Analytical Methods

Accepted Manuscript

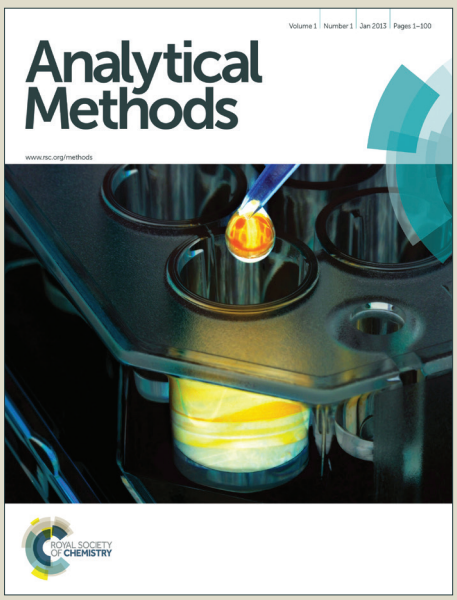

ROYAL SOCIETY OF CHEMISTRY

www.rsc.org/methods

Cite this: DOI: 10.1039/c0xx00000x

www.rsc.org/xxxxxx

FULL PAPER

Peptide nucleic acid label-free biosensor for Mycobacterium Tuberculosis DNA detection *via* azimuthally-controlled grating-coupling SPR

Davide Silvestri,[a]* Agnese Sonato,[b,d] * Gianluca Ruffato,[b,c] Anna Meneghello,[e,g] Agnese Antognoli,[e] Erica Cretaio,[e] Monica Dettin,[f] Annj Zamuner,[f] Elisabetta Casarin,[a] Gabriele Zacco,[c,d] Filippo Romanato,[b,c,d] and Margherita Morpurgo[a]

Received (in XXX, XXX) Xth XXXXXXXXX 20XX, Accepted Xth XXXXXXXXX 20XX

DOI: 10.1039/b000000x

Grating Coupled Surface Plasmon Resonance phenomena under azimuthally control of the incident light (φ≠0° GC-SPR) have recently been exploited for the development of biosensing solutions with a sensitivity similar to that of classic prism-coupled SPR sensors, with the advantage of higher miniaturization potential. Here we combined the use of φ≠0° GC-SPR with the use of peptide nucleic acid (PNA) probes and a strategy for maximizing the signal-to-noise ratio for the sensitive detection of *Mycobacterium tuberculosis* (MT) DNA. We focused the attention on the optimization of the PNA-based sensing layer by controlling the sensing surface composition with the PNA-based probe and a poly(ethylene oxide) (PEO)-based antifouling layer. We tested the sensor response firstly in the presence of complementary and non-complementary oligonucleotides, and then we applied our strategy to the detection of PCR amplified samples, using the fluorescence-based microarray technology as control. With the φ≠0° GC-SPR set-up adopted, a limit of detection (LOD 0.26 pM) more than one order of magnitude lower than that registered for the fluorescence method (LOD 8.9 pM) was observed using complementary oligonucleotides target. Also when PCR amplicons were analysed on SPR grating surfaces, lower DNA concentrations were detectable with the SPR readout as compared to the fluorescence one, and with an experimental protocol that does not include the need to use expensive fluorophore molecules. The whole approach, involving the sensor fabrication, the sensing surface control and DNA detection has demonstrated that φ≠0° GC-SPR is a good starting point for a sensitive, versatile and scalable biosensing technique, that will be further investigated in future experiments.

Introduction

Among the most advanced sensing technologies currently explored for the detection of low concentrated bioanalytes, one of the most investigated is the label-free Surface Plasmon Resonance (SPR) technique.[1-4] The most common SPR based configuration (e.g in the Biacore® instrumentation) is the one that adopts a prism to promote Surface Plasmon Polariton (SPP) coupling with the incident light (Kretschmann-Raether or Prism Coupling SPR – PC-SPR).[2, 5-7]

Alternative configurations are available which are more suitable for instrumental miniaturization and for multiplexing. However, these configurations, which bypass the use of the prism by adopting nano-grated metal surfaces (Grating Coupled SPR, GC-SPR) to allow the coupling of the incident light with SPPs, [4] are less sensitive in terms of RIU (refractive Index Unit). [8]Nevertheless, GC-SPR sensing performances can be improved by almost one order of magnitude by modifying the traditional SPR configurations (i.e. prism-coupling or null azimuth – φ=0° – grating-coupling methods) to azimuthally-rotated GC-SPR (φ≠0° GC-SPR)[9]. As demonstrated through its first application in simple chemical systems[10, 11] GC-SPR under azimuthal control, gives sensitivities up to 600 and 800°/RIU, which are significantly higher than ones obtained by using standardGC- and PC-SPR methods (typically 50–150°/RIU).[12] The sensitivity enhancement mechanism is attributed to the fact that the azimuthal orientation of the sinusoidal grating induces a double surface plasmon polariton (SPP) excitation with a single incident wavelength. Due to the resulting symmetry breaking, polarization assumes a fundamental role on SPPs excitation, and it must be properly tuned in order to optimize the coupling strength. The

sensitivity improvement given by the employment of azimuthally-rotated GC-SPR was previously demonstrated in theoretical[9, 11] and experimental works including both model of simple biochemical interactions, like the biotin-avidin binding, [13-16]and, more recently, reactions of clinical relevance like the detection of cystic fibrosis (CF) DNA.[17] The possibility to identify the presence of specific genomic sequences directly within complex biological samples is of great interest in different fields, including the diagnosis of infection diseases, such as Tuberculosis (TB). TB remains a major global health problem, responsible for ill health among millions of people every year. According to WHO data for 2014,[18] TB ranks as the second leading cause of death from an infectious disease worldwide, after the human immunodeficiency virus (HIV). Estimates indicate that there were 9.0 millions new TB cases in 2013 and 1.5 million TB deaths (1.1 million among HIV-negative people and 0.4 million among HIV-positive people). Globally, 3.5% of new and 20.5% of previously treated TB cases were estimated to have had MDR (Multi Drug Resistant) TB. In 2013, 136000 of the estimated 300000 MDR-TB patients who could have been detected were diagnosed and notified. This was equivalent to almost one in two (45%), and up from one in six in 2009. This result is related to the progress in the detection of drug-resistant TB that was facilitated by the use of new rapid diagnostics.

Following recent breakthroughs in TB diagnostics, the use of rapid molecular tests to diagnose TB and drug-resistant TB is increasing. However, till now, the most common TB diagnosing method worldwide is sputum smear microscopy, and only in countries with more developed laboratory capacity, TB is diagnosed via microbiological culture that is recognised as the current reference method. Many new diagnostic technologies are under development[4, 19] but WHO estimates that the funding required to rapidly evaluate whether these tests are accurate and ready for implementation is far from adequate.[18] Starting from these considerations, other approaches, alternative or complementary to the methods currently adopted, should be explored in order to fulfil the biosensing requirements of sensitivity, speed of analysis, low costs and system miniaturization. The use of surface plasmon resonance (SPR) and nucleic acid-based sensing has demonstrated to be a good starting point for the development of novel MT DNA detection approaches.[20, 21]

In this work we investigated the employment of a Peptide Nucleic Acid (PNA) probe anchored on the azimuthally-controlled GC-SPR ellipsometer for MT sensing, using reading parameters previously optimized in our laboratory. [12, 16]

PNAs are synthetic nucleic acid analogues with uncharged backbone, that bind to the complementary nucleic acid sequence with higher affinity than their natural analogues (i. e. DNA or RNA)[22-24]. The presence of an uncharged backbone reduces the stand-strand repulsion associated to DNA/DNA or DNA/RNA complexes and makes PNAs useful probes when detecting low concentrated analytes [25-29]. As sensing probe, we chose a 15-mer PNA sequence matching a fragment of the MT RpoB gene, whose mutations are involved in the resistance to the antibacterial agents of the rifampicin family.[30]

Initially, the efficiency of the system as a function of chemistry of the sensing layer was tested by comparing the use of thiolated-PNA (HS-PNA) or a thiolated-poly(ethyleneoxide-5KDa)-PNA (HS-PEO_{5KDa}-PNA) as probes anchored on the SPR sensing surface, whose antifouling property was ensured by using a 2KDa thiolated-PEO (HS-$mPEO_{2KDa}$) as backfilling element[16].

The sensing layer composition, in terms of HS-PEO and HS-PEO-PNA or HS-PNA quantities, was tuned in order to optimize the sensor response We developed a one-step surface dressing protocol based on Langmuir adsorption kinetics[31, 32] through which we were able to control the final surface composition in terms of probe and backfiller ratio, and the final sensing event was performed in the presence of complementary oligonucleotides or PCR amplicons, to mimic more complex clinical samples. The SPR data were also compared to those generated with a microarray fluorescence-based system.

Materials and Methods

2.1. Chemicals and solutions

All chemicals and solution components were purchased from Sigma Aldrich (St. Louis, MO, USA) if not otherwise specified. The composition of the buffers used is: *SSC buffer 20X*: 3 M sodium chloride, 300 mM trisodium citrate, pH 7.0; *microarray printing buffer 6X*: 300 mM sodium phosphate, 0.02% triton, pH 8.5; *microarray blocking solution*: 0.1 M Tris, 50 mM ethanolamine, pH 9; *microarray washing solution*: 4X SSC, 0.1% SDS; *Phosphate Buffer Saline (PBS)*: 137 mM NaCl, 2.7 mM KCl, 10 mM Na_2HPO_4, 1.8 mM KH_2PO_4, pH 7.4. The water used in all experiments was of double-distilled (dd-H_2O) or milliQ grade.

2.2. Probes, backfiller and DNA targets

H-Cys-$(CTGTCGGCGCTGGGG)_{PNA}$-$(Lys)_4$-NH_2 (**HS-PNA**), Fmoc-Cys(Trt)-PEO_{5KDa}-$(CTGTCGGCGCTGGGG)_{PNA}$-Ala-Ala-$CONH_2$ (**HS-PEO_{5KDa}-PNA**) and α-Cys(Trt),ω-methoxy PEO_{2KDa} (**HS-$mPEO_{2KDa}$**) were synthesized according to protocols described elsewhere. [16, 33]

The DNA probe for glass functionalization (5'-$H_2N(CH_2)_6$-CTGTCGGCGCTGGGG-3'$_{DNA}$, **H_2N-DNA-p**), the probe-complementary sequence (5'-CCCCAGCGCCGACAG-3', **DNA-c**), its 5' Cy3 labelled analogue (5'-Cy3-CCCCAGCGCCGACAG-3', **Cy3-DNA-c**), the non-complementary sequence (5'-AGCTGTGTCTGTAAACTGATGG-3', **Cy3-DNA-nc**) and its Cy3 labelled analogue (5'-AGCTGTGTCTGTAAACTGATGG-3', **Cy3-DNA-nc**) were purchased from IDT Integrated DNA Technologies (Leuven, Belgium). Wild type MT 224 bp PCR amplicon (**PCR amplicon**) and its Cy3 labelled (**Cy3-PCR amplicon**) analogue were obtained (Supplementary Information - S.I.) from a *Mycobacterium* (MT) DNA extract from a wild type strain, kindly provided by Professor Riccardo Manganelli (University of Padova).

2.3. Flat and nanostructured substrates

Plasmonic surfaces consisted of a thiolene resin (NOA61 - Norland products NOA61, Las Vegas, NV, USA) sinusoidal grating (500 nm period, 40 nm amplitude) supported onto a glass-slide and coated by a bi-metallic layer (Chromium (5 nm)/Gold (40 nm)) through thermal evaporation. Substrates were produced combining laser interference lithography with soft lithography

according to a procedure described elsewhere. [12, 16, 17, 34]

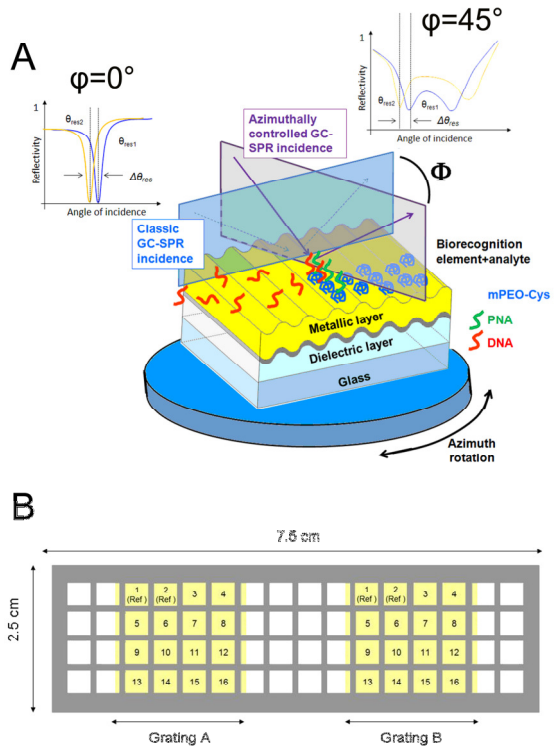

Figure 1. Cartoon (not in scale) summarizing the experimental set-up. (A) The azimuthally-controlled GC-SPR platform. A monochromatic collimated light is impinged upon the nanostructured surface and the intensity of the reflected light is registered as a function the incident angle. In the classic configuration or null-azimuth (φ=0°), the incident light plane is perpendicular to the grating ridge direction. In the φ≠0° configuration, the grating plane is rotated to a different value, in our case by 45°. (B) Slide holding two nanogratings (yellow), integrated with a 64 wells ProPlate mask (grey) to generate 16x2 isolated grating-exposing wells. Two regions in each grating are kept un-functionalized and used as references in the measurements. The image is adapted from [12]

Grating geometry chosen was previously optimized through theoretical simulations of SPPs coupling on metallic gratings based on Chandezon's method,[35, 36] with the aim of obtaining the optimal SPR response in terms of surface reflectivity, SPP resonance angle and sensitivity.[37]

Flat gold surfaces adopted for fluorescence tests consisted of microscope glass-slides coated by a bi-metallic Chromium (5 nm)/Gold (40 nm) layer deposited by thermal evaporation. Gold flat and grating surfaces were functionalized and hybridized using ProPlate masks to create multiple incubating chambers (Grace Bio-Labs ProPlate® microarray system with 16 or 64 wells, Sigma Aldrich). Amine-reactive microarray glass-slides (25 × 75 mm) were purchased from LifeLineLab (Pomezia, Italy).

2.4. SPR measurements

A J.A. Woollam Co. VASE ellipsometer was used for SPR measurements (Lincoln, NE, USA). The instruments is characterized by an optical bench for focusing and polarization control of the output light, a gating monochromator, located in sequence to a Xe-Neon 75 W lamp, a sample holder for the vertical mounting of the sample, a rotating goniometer for incidence angle scan, and a detector. The angular and wavelength spectroscopic resolution of the instrument is 0.005° and 0.3 nm, respectively. All measurements were performed by angular scanning in the dry state, after each experimental step. For the considered rotated-azimuth configuration, the incident wavelength λ was set to 625 nm, the azimuthal angle (φ) to 45°, using a goniometer with a precision of 5' mounted onto the sample holder, and the incident light polarization (α) was tuned to the value of 140° in order to optimize the depth of the resonance dip (α = 0° corresponding to TM polarization). Wavelength, azimuth and polarization, as they are correlated parameter, were chosen in order to optimize both the angular sensitivity and the reflectivity dip curve amplitude using Chandezon's method simulations.[36] For instance, when passing from null (φ=0°) to φ=45°, a 8-fold instrumental sensitivity increase was shown.[12] In addition in the azimuthally rotated GC-SPR TM polarization is no longer the optimal one for SPP excitation, and the polarization angle α should be tuned accordingly to the formula α =180°-tan-1(tanφ cosθ), derived elsewhere[38], θ being the resonance polar angle. The incidence polar angle ranged from 20° to 80° by a step of 0.2°. Reflectivity minima were derived by fitting the reflectivity curves with a Lorentz function and the resonance angle shifts were subsequently calculated. (**Figure 1**).

2.5. Fluorescence measurements

Fluorescent measurements on hybridized arrays were performed using GenePix 4000B laser scanner and software (Molecular Devices, Sunnyvale, CA) using 532 nm wavelength. Fluorescent spot intensities were quantified after normalizing the data by subtracting local background from the recorded spot intensities. The mean and standard deviation were calculated for each set of triplicate sub-array, consisting in a 4x4 spot array.

2.6. Sinusoidal surface dressing setup and functionalization for SPR readouts

Seven solutions of SH-PEO_{5KDa}-PNA/SH-mPEO_{2KDa} backfiller or HS-PNA/SH-PEO_{2KDa} backfiller were tested for surface dressing setup. Based on the thiol adsorption kinetics theory, [31, 32] we derived a predictive calculation reported in detail in the supplementary information (S.I.) which permits to control and tune the adsorption of thiolated species onto gold surfaces when adopting a co-deposition procedure. With the help of the Wolfram Mathematica software, we calculate the concentrations of probe and backfiller to be adopted in the co-deposition (24h hour contact) process so to generate different surface probe:backfiller ratios (namely 1:0; 0.43:0.57; 0.2:0.8; 0.1:0.9; 0.05:0.95; 0.02:0.98; 0:1). The deposition kinetic constants of all the thiolated species necessary for the mathematical elaboration[31, 32] were determined experimentally beforehand, as described in the S.I.

The thiol function of probes and backfiller molecules, which were obtained by chemical synthesis, [16, 33] were available with a trityl (trt) residue to prevent unwanted oxidation which could lead to less predictable gold deposition kinetics. In order to generate the desired deposition mixtures, stock solutions of trt-protected PNA probe and backfiller were properly diluted, mixed and vacuum dried. Prior to deposition, the trt protective was cleaved by dissolving the dried mixtures in the minimum amount of TFA for 15 minutes (min.) at room temperature[16, 33]; dd-H_2O was added to

reach the appropriate final concentration of 1 mM thiol. Mixtures were vortexed thoroughly and the insoluble triphenylmethane was removed by centrifugation and solutions were deposited (40 µL or 300 µL/chamber for 64 or 16-well masks, respectively) for 24h at 35°C and 75% relative humidity on the gold surfaces, which had been pre-treated (10 min.) in basic piranha solution (dd-H_2O:H_2O_2:NH_4OH in a 5:1:1 ratio), rinsed in dd-H_2O, dried under N_2 flux and inserted into the multiwells masks (ProPlate, Sigma Aldrich). After deposition, surfaces were rinsed thoroughly with dd-H_2O, dried under nitrogen (N_2) stream and in vacuum.

To assess noise due to non specific DNA pairings, the results from the incubation with DNA-c were compared to those given by the DNA-nc ones; BSA-related shifts were used as to estimate the antifouling property of the system from protein elements, i.e. use of BSA - containing diluent buffers. The S/N (signal to noise) ratio (S/N) was calculated from the ratio between the signals generated by the complementary and non-complementary DNAs after the 2 hours of incubation. The optimized probe:backfiller ratio defined in these experiments was selected for all other SPR surface functionalizations and SPR measurements.

2.7. Functionalization of flat gold and glass surfaces for fluorescent readouts

Fluorescent readout experiments were performed on flat gold surfaces or microarray glass-slides. Probe solutions were deposited in spots using the VersArray Chip Writer Pro System (Biorad, Hercules, CA), with Telechem SMP3 microspotting pins (Arrayit Corporation, Sunnyvale, CA).

When using flat gold substrates, solutions and deposition conditions were as defined from the results of the dressing protocol setup experiments. Spot functionalized surfaces were further blocked with BSA 2% for 45 min., rinsed with PBS 1 X, milliQ water and N_2 flux dried.

When using microarray glass-slides, a 20 µM solution of NH_2-DNA-p in 1.5X *microarray printing buffer* was incubated overnight at 75% humidity. Surfaces were blocked and washed with *microarray blocking* and *washing solutions* as indicated by the glass-slide supplier.

Both for flat gold surfaces and glass surfaces deposited through microarray spotter, the described blocking step after probe deposition was included since spots dimension is of 100 µm and thus most part of the sensing surface is unfunctionalized and need to be therefore passivated prior to hybridization experiments.

2.8. DNA hybridization protocols

All surface dressing, hybridization procedures and measurements were performed in duplicate so that the final results obtained are an average value between all the experiment replicas.

Hybridizations were performed using the Array Booster AB410 hybridization station (Advalytix, Munich, Germany) in optimized buffer and temperature conditions for MT target sequence detection.

Along the surface dressing selection experiments, hybridization was carried out with DNA-c or DNA-nc (1 µM in SSC buffer 1X) or 1 mg/ml BSA in PBS for 1h at 35°C plus 1h at 50°C. After each incubation step, surfaces were rinsed thoroughly with dd-H_2O and dried under N_2 stream, before SPR measurements.

In the SPR and fluorescence sensitivity experiments, surfaces were incubated at 50°C with either DNA-c or Cy3-DNA-c (between 10nM to 3.2pM in 1X SSC, 0.1% SDS, 0.02% BSA, 2h), or the PCR amplicon, or Cy3-PCR amplicon (between 10nM to 16 pM in 4X SSC, 0.1% SDS, 0.02 % BSA, 3h). Hybridizations were carried out after denaturing the samples for 5 min. at 95°C followed by cooling on ice. After hybridization, slides were washed in the Advawash Station AW400 (Advalytix) (5 min. in 1X SSC 0.1% SDS at 50°C, 2min. in 0.2X SSC, 2 min. in 0.1X SSC and 30 s in dd-H_2O), dried under N_2 or using a Microarray High-Speed Centrifuge (Arrait Corporation, Sunnyvale, CA). From calibration curves obtained in the sensitivity experiments on SPR gratings or microarray slides, the limit of detection (LOD) and limit of quantification (LOQ) were calculated: LOD is defined as 3 σ whereas LOQ is defined as 10 σ, where σ is the standard deviation of the blank experiment.

3. Results and Discussion

3.1. Identification of the best performing surface coating

Considering that the quality of a sensor is related to both analyte-specific and non analyte-related signal intensities, preliminary experiments were necessary to identify the best probe for our purposes and its optimal density on the surface. In principle, considering that the SPP electromagnetic field decays exponentially when passing from the metal/dielectric interface to the dielectric medium, the SPR response intensity related to a non PEGylated HS-PNA probe should lead a stronger signal than that generated with the PEO-spaced one. On the other hand, the PEO spacer of the SH-PEO_{5KDa}-PNA probe could both favour accessibility of the probe for the analyte and complement the antifouling activity exerted by the 2KDa PEO backfiller. In addition, the probe efficiency in capturing the analyte depends also on its surface density due to steric factors. Keeping in mind the above reasoning, different sensing surfaces were deposited using either the HS-PNA or the HS-PEO_{5KDa}-PNA probes, diluted to different extent with the antifouling (or backfiller) HS-$mPEO_{2KDa}$, choosing probe:backfiller ratios from 1 to 0.05 (**Figure 2**). The amount of each surface-tethered element was varied by changing the composition of the binary mixture used in the one-step deposition process, following a calculation based on the Langmuir adsorption kinetics[31, 32] and described in the Supporting Information (S.I.). The φ≠0°-GC-SPR signal was collected after incubating all the prepared surfaces either in DNA-c (Signal), or DNA-nc (Noise) or BSA (a model for protein-derived interfering elements).

Using both types of probes (HS-PNA or HS-PEO_{5KDa}-PNA), the highest SPR output generated by DNA-c was obtained for the 0.1 probe surface coverage fraction (**Figure 2**). For coverage fractions smaller than 0.1, the SPR output diminished with the PNA content, as expected for a reduced capacity of the surface towards the analyte binding, due to a decrease in probe availability.

On the contrary, for coverage fractions higher than 0.1 we observed an inverse correlation between the amount of probe and signal, indicating that at higher PNA content, the probe molecules packing is too high, impairing the ability of the target DNA to hybridise with them.

The surfaces functionalised with the smaller HS-PNA probe

yielded higher SPR signals than those containing the PEGylated probe

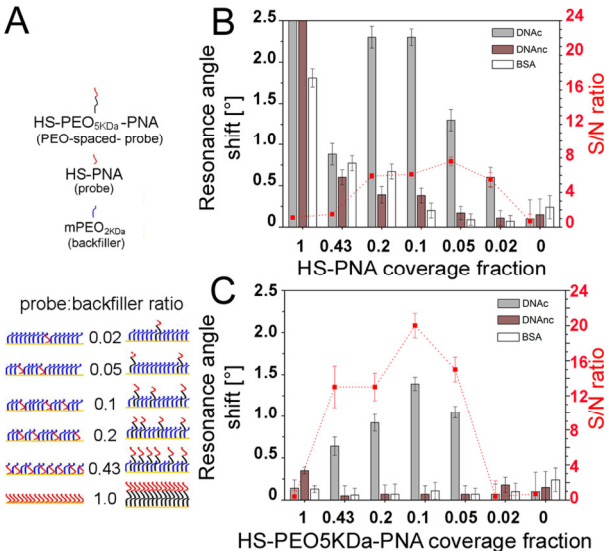

Figure 2. SPR signal as a function of surface composition Cartoon depicting the different surface coatings (**A**) and resonance angle shifts obtained on gratings functionalized with different relative ratios of HS-PNA+HS-mPEO2KDa (**B**) and HS-PEO_{5KDa}-PNA+HS-$mPEO_{2KDa}$ (**C**), upon incubation in 0.1% BSA in PBS (white bars), 1µM DNA-nc (brown bars) and 1µM DNA-c (grey bars). The S/N ratios calculated for each surface are also reported (red dotted curves). All measurements were done in duplicate. The error bar represents the standard deviation of the resonance angle shifts collected.

This is likely due to the fact that using the shorter probe the analyte gets closer to the plasmonic surface.

On the other hand, the HS-PNA dressed surfaces, at all tested probe:backfiller ratios, suffered from quite relevant non-specific interactions with both kind of non-specific target elements (DNA-nc or BSA). In the case of the HS-PEO_{5KDa}-PNA surfaces instead, non-specific interactions were observed only at HS-PEO_{5KDa}-PNA coverage fraction of 1. These results suggested that when PNA is in close proximity to the surface (e.g. with the HS-PNA probe), it interferes with an efficient packing of the PEO backfiller, reducing its antifouling property. However, when properly spaced by the long PEO chain, the PNA molecules do not interfere with the formation of the protecting layer and the PEO spacer, being of the same chemical nature as the HS-$mPEO_{2KDa}$ backfiller, contributes to the antifouling layer formation. The advantage of using the HS-PEO_{5KDa}-PNA probe instead of the smaller HS-PNA becomes more evident when comparing the Signal to Noise values (S/N) (**Figure 2**). The highest S/N (19.05) was obtained for the 0.1 coverage fraction of HS-PEO_{5KDa}-PNA, resulting 2.5 fold higher than the one obtained with the best performing HS-PNA containing surface (7.65 for the 0.05 coverage fraction). Starting from these results, the sensing surface coated by HS-PEO_{5KDa}-PNA at the 0.1 coverage fraction was selected for all the sensing experiments.

3.2. Detection of MT DNA oligonucleotides

Table 1 summarizes the readout intensities obtained with the three analytical methods explored. The signal measured on the gold substrate was much lower than that measured using the glass surface, likely due a fluorescence quenching effect exerted by gold (see also S.I.).

Table 1. Measurement outputs from MT DNA-c hybridization experiments on microarray glass or gold slides for fluorescence readouts and gold gratings for SPR readouts.

Probe	DNA		PEO_{5KDa}PNA:$_{PEO2KDa}$ (0.1:0.9)
Surface type	Glass array slide	Flat Gold	Sinusoidal grating
[DNAc] nM	Fluorescent signal intensity (A.U.)		φ≠0 GC-SPR angle shift (°)
10	31826.13±4144.13*	148.25±25.2*	0.68±0.1*
2	24002.38±5472.95*	121.5±31.84*	0.74±0.15*
0.4	8715.63±1566.26*	11.0±2.16	0.40±0.03*
0.08	485.75±27.98*	6.50±2.08	0.22±0.03*
0.016	85.63±29.37*	1.75±0.5	0.21±0.01*
0.0032	20.88±10.25	5.75±0.96	0.11±0.02*
0	24.25±1.71	2.00±0.82	0.02±0.01

Significant positive readings are marked with (*)
A.U.: arbitrary unit

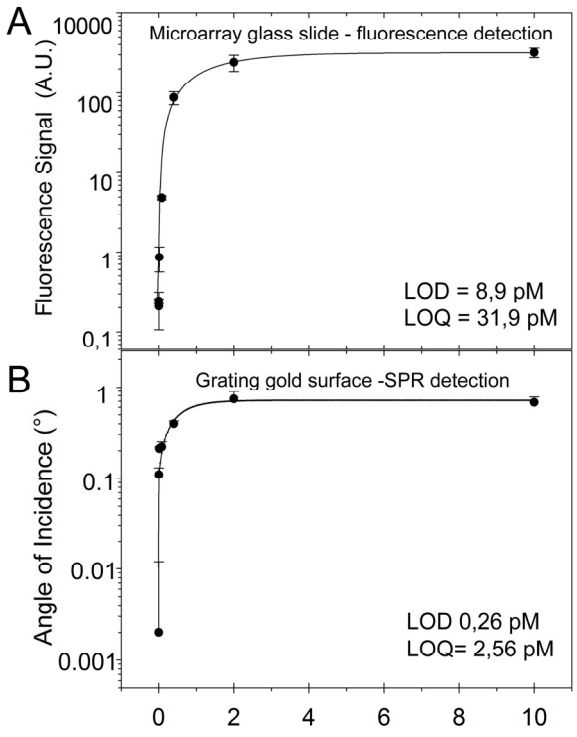

Figure 3. Comparison between fluorescence (A) and GC-SPR (B) detection of DNA-c (5'-Cy3 labeled in the case of fluorescence measurement). Readouts from 10 nM to 0 nM were interpolated in a tendency curve for LOD and LOQ calculation.

For comparing the SPR detection with the results obtained on microarray glass slides, two calibration curves were plotted as function of the target concentration to calculate the limit of detection (LOD) and the limit and quantification (LOQ) (**Figure 3**).Using the SPR measurement, the calculated LOD for complementary MT oligonucleotide was of 0.26 pM, which is more than 30 times lower than that registered by the fluorescence-based method (8.9 pM).

A

Analytical readouts of PCR amplified MT DNA fragment

	Fluorescent intensity (A.U.)	SPR angle shift (°)
[Amplicon] nM		
10	1573.25±115.95	1.51±0.04
0.4	26.5±2.0	1.40±0.02
0.016	13.64±1.3	0.83±0.07
0	7±0.82	0.02±0.01

B

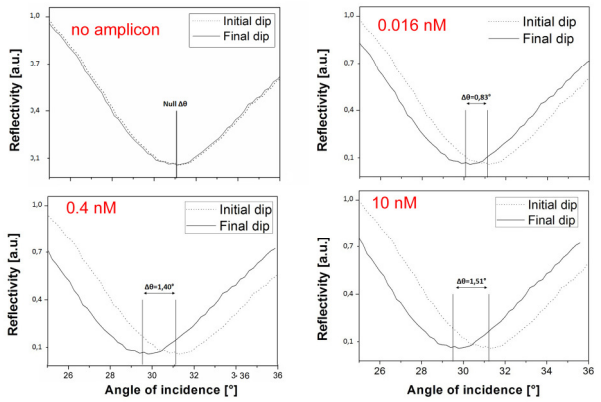

Figure 4. GC-SPR and fluorescent detection of the PCR-amplified MT DNA fragment. (**A**) Analytical readouts obtained in the detection of a PCR-amplified MT DNA fragment using the fluorescence based sensing technology on glass microarrays and the SPR instrumentation. (**B**) SPR reflectivity dips before (dotted lines) and after surface hybridization (solid lines) of the different amplicon concentrations.

The LOQ for SPR detection was of 2.56 pM while for the fluorescence readouts, it was one order of magnitude higher (31.9 pM), again demonstrating the lower sensing detection limits of the SPR sensing. The sensitivity displayed by the fluorescence set up is in line with the theoretical limits identified in a similar microarray configuration which set the LOD of Cy3-labelled DNA at about 15000 molecules/μm^2.[39] On the other hand, the sensitivity of the SPR system for the oligo DNA is more than 10 fold higher than that registered with classic SPR sensors using PNAs as probes, for which the LOD was estimated in the nM range and of the same order as that obtained upon eith gold NP or polymer based amplification strategies. [3, 27, 40]

3.3. Sensing PCR amplified *Mycobacterium* DNA

The optimized SPR platform was also tested to detect a PCR amplified fragment (224 bp) of the MT genome (**Figure 4**), to evaluate the system response in the presence of a more complex DNA sequence if compared to perfectly match short oligonucleotide. When incubating PCR amplicons for plasmonic SPR detection, resonance shifts are higher than the ones registered by hybridizing DNA-c, likely due to the greater dimension of the PCR fragment with respect to the oligonucleotide. A positive correlation between analyte concentration and resonance angle shift, with significant signal readouts, was obtained at all tested concentrations, down to 16 pM. The signal intensity registered at 16 pM (0.83±0.07°) is 40-fold higher than that generated by 0 nM negative control (0.02±0.01°), indicating that higher dilutions with lower DNA content could be investigated. When the same amplicon dilutions were probed with the fluorescent microarray method, the lowest significant readout (signal intensity at least 2-fold higher than that generated by the 0 nM negative control) was obtained at 0.4 nM analyte concentration (**Figure 4.A**).

Even if the LOD/LOQ for the PCR amplicon were not estimated in these experiments, similarly to what observed with the smaller oligonucleotide analyte, the sensitivity registered with the φ≠0 GC-SPR set-up is of the same order of magnitude as that registered with classic PNA-probe PC-SPR systems only upon their implementation with complementary amplification strategies[27, 40] or when the large genomic DNA is the analyte[21]. Notably, such amplification strategies[20, 41-48] are at all compatible with our φ≠0 GC-SPR system so that, in principle, the sensitivity limits can be further reduced.

Conclusions

The whole approach, involving fabrication, surface chemistry control and sensor configuration, demonstrated that φ≠0° SPR sensing is a technique applicable to the detection of low MT related DNA species at concentrations below the pM range. This sensitivity range is of the same order as that achieved with classic PC-SPR set-ups only when these are complemented with nanoparticle- or polymer- based amplification solutions. It is worth noticing that, besides the high sensitivity, the independence of the present configuration from the use of the prism for SPP coupling makes it more prone to miniaturization than the classic PC-SPR based solutions.

In principle, this approach is applicable as alternative or as a complementary tool to the traditionally employed sensing methodologies, with advantages in terms of time of analysis and cost, since no labelling procedures are necessary.

Future experiments will include the evaluation of the system performance in the presence of more complex artificially contaminated samples and unprocessed or minimally processed clinical samples, and the possibility to distinguish single point DNA mutations as those involved in TB MDR.

In addition, research is underway to integrate the detector in a lab-on-a-chip diagnostic prototype with temperature and microfluidic control, which could be suitable for multiplex analysis.

Finally, we would like to point out that the high sensitivity here achieved derives from the synergic effect exerted by the azimuthally-controlled grating-coupled SPR and the optimised antifouling/PNA probe coating. To our knowledge, this is the first time that a quantitative correlation between surface composition and S/N is shown. The results stem from the contribution of both theory-driven hardware implementation and the *ad-hoc* designed surface chemistry. This demonstrates the importance of implementing multidisciplinary approaches for better results.

Acknowledgments

This work was supported by a grant from Materials Science and Engineering PhD and Molecular Sciences PhD Schools of University of Padova and the Strategic project of University of Padova "PLATFORMS".

The authors thank Professor Riccardo Manganelli (University of Padova) for providing DNA extract from a wild type strain of *M.*

tuberculosis.

Notes and references

[a] *University of Padova, Department of Pharmaceutical and Pharmacological Sciences, Via Marzolo 5, 35131 Padova (Italy)*
[b] *University of Padova, Department of Physics, Via Marzolo 8, 35131 Padova (Italy)*
[c] *LaNN Laboratory for Nanofabrication of Nanodevices, Corso Stati Uniti 4, 35127 Padova (Italy); Veneto Nanotech S.C.p.A.*
[d] *IOM-CNR, Area Science Park, 34149 Basovizza (Italy)*
[e] *Nanofab – NanoFabrication Facility Via delle Industrie 5, 30175 – Venezia Marghera 30174 Venezia (Italy); Veneto Nanotech S.C.p.A.*
[f] *University of Padova, Department of Industrial Engineering, Via Marzolo, 9, 35131 Padova (Italy)*
[g] *University of Padova, Department of Biology, Via U. Bassi,58/B, 35131 Padova (Italy)*

* These authors contributed equally to the work
Corresponding authors: margherita.morpurgo@unipd.it; filippo.romanato @unipd.it

† Electronic Supplementary Information (ESI) available: [1. therory and experimentals for the control of the surface chemistry composition; 2. Comparison between glass substrate-based and gold substrate-based fluorescence DNA hybridization experiments; 3. Preparation of MT PCR amplicons]. See DOI: 10.1039/b000000x/

1. J. Homola, *Chem Rev*, 2008, **108**, 462-493.
2. S. A. Maier, *Plasmonics: Fundamentals and Applications*, XXVI edn., Springer, New York, NY, 2007.
3. H. Sipova and J. Homola, *Anal Chim Acta*, 2013, **773**, 9-23.
4. A. P. F. Turner, *Chem Soc Rev*, 2013, **42**, 3184-3196.
5. E. Kretschmann and H. Raether, *Zeitschrift für Naturforschung*, 1968, **23a**, 2135-2136.
6. R. L. Rich and D. G. Myszka, *J Mol Recognit*, 2007, **20**, 300-366.
7. R. L. Rich and D. G. Myszka, *Anal Biochem*, 2007, **361**, 1-6.
8. J. Homola, I. Koudela and S. S. Yee, *Sensor Actuat B-Chem*, 1999, **54**, 16-24.
9. G. Ruffato, E. Pasqualotto, A. Sonato, G. Zacco, D. Silvestri, M. Morpurgo, A. De Toni and F. Romanato, *Sensor Actuat B-Chem*, 2013, **185**, 179-187.
10. F. Romanato, K. H. Lee, H. K. Kang, G. Ruffato and C. C. Wong, *Opt Express*, 2009, **17**, 12145-12154.
11. G. Ruffato, G. Zacco and F. Romanato, in *Plasmonics - Principles and Applications*, ed. K. Y. Kim, Intech, 2012, pp. 419-444.
12. A. Sonato, G. Ruffato, G. Zacco, D. Silvestri, M. Natali, M. Carli, G. Giallongo, G. Granozzi, M. Morpurgo and F. Romanato, *Sensor Actuat B-Chem*, 2013, **181**, 559-566.
13. A. Cattani-Scholz, D. Pedone, F. Blobner, G. Abstreiter, J. Schwartz, M. Tornow and L. Andruzzi, *Biomacromolecules*, 2009, **10**, 489-496.
14. L. A. Chrisey, G. U. Lee and C. E. O'Ferrall, *Nucleic Acids Res*, 1996, **24**, 3031-3039.
15. P. Gong, C. Y. Lee, L. J. Gamble, D. G. Castner and D. W. Grainger, *Anal Chem*, 2006, **78**, 3326-3334.
16. A. Sonato, D. Silvestri, G. Ruffato, G. Zacco, F. Romanato and M. Morpurgo, *Applied Surface Science*, 2013, **286**, 22-30.
17. A. Meneghello, A. Antognoli, A. Sonato, G. Zacco, G. Ruffato, E. Cretaio and F. Romanato, *Analytical Chemistry*, 2014, **86**, 11773-11781.
18. W. H. O. (W.H.O.), *Global Tuberculosis Report*, 2014.
19. S. D. Lawn, P. Mwaba, M. Bates, A. Piatek, H. Alexander, B. J. Marais, L. E. Cuevas, T. D. McHugh, L. Zijenah, N. Kapata, I. Abubakar, R. McNerney, M. Hoelscher, Z. A. Memish, G. B. Migliori, P. Kim, M. Maeurer, M. Schito and A. Zumla, *Lancet Infect Dis*, 2013, **13**, 349-361.
20. H. X. Chen, F. Liu, K. Koh, J. Lee, Z. H. Ye, T. T. Yin and L. Z. Sun, *Microchim Acta*, 2013, **180**, 431-436.
21. N. Prabhakar, K. Arora, S. K. Arya, P. R. Solanki, M. Iwamoto, H. Singh and B. D. Malhotra, *Analyst*, 2008, **133**, 1587-1592.
22. M. Egholm, O. Buchardt, P. E. Nielsen and R. H. Berg, *Journal of the American Chemical Society*, 1992, **114**, 1895-1897.
23. P. E. Nielsen, *Chem Biodivers*, 2010, **7**, 786-804.
24. P. E. Nielsen, M. Egholm, R. H. Berg and O. Buchardt, *Science*, 1991, **254**, 1497-1500.
25. Z. Q. Gao, S. Rafea and L. H. Lim, *Adv Mater*, 2007, **19**, 602-+.
26. M. Steichen, Y. Decrem, E. Godfroid and C. Buess-Herman, *Biosens Bioelectron*, 2007, **22**, 2237-2243.
27. X. Su, H. F. Teh, K. M. Aung, Y. Zong and Z. Gao, *Biosens Bioelectron*, 2008, **23**, 1715-1720.
28. X. Su, H. F. Teh, X. Lieu and Z. Gao, *Anal Chem*, 2007, **79**, 7192-7197.
29. A. I. K. Lao, X. D. Su and K. M. M. Aung, *Biosensors & Bioelectronics*, 2009, **24**, 1717-1722.
30. M. T. McCammon, J. S. Gillette, D. P. Thomas, S. V. Ramaswamy, E. A. Graviss, B. N. Kreiswirth, J. Vijg and T. N. Quitugua, *Antimicrob Agents Ch*, 2005, **49**, 2200-2209.
31. K. Hu and A. J. Bard, *Langmuir*, 1998, **14**, 4790-4794.
32. D. S. Karpovich and G. J. Blanchard, *Langmuir*, 1994, **10**, 3315-3322.
33. M. Dettin, D. Silvestri, R. Danesin, E. Cretaio, G. Picariello, E. Casarin, A. Sonato, F. Romanato and M. Morpurgo, *Molecules*, 2012, **17**, 11026-11045.
34. G. Zacco, F. Romanato, A. Sonato, D. Sammito, G. Ruffato, M. Morpurgo, D. Silvestri, M. Carli, P. Schiavuta and G. Brusatin, *Microelectronic Engineering*, 2011, **88**, 1898-1901.
35. J. Chandezon, G. Raoult and D. Maystre, *Journal of Optics*, 1980, **11**, 235-241.
36. F. Romanato, H. K. Kang, K. H. Lee, G. Ruffato, M. Prasciolu and C. C. Wong, *Microelectron Eng*, 2009, **86**, 573-576.
37. J. Dostalek, J. Homola and M. Miler, *Sensor Actuat B-Chem*, 2005, **107**, 154-161.
38. F. Romanato, K. H. Lee, G. Ruffato and C. C. Wong, *Appl Phys Lett*, 2010, **96**.
39. J. S. Lee, J. J. Song, R. Deaton and J. W. Kim, *Biomed Res Int*, 2013.
40. H. A. Joung, N. R. Lee, S. K. Lee, J. Ahn, Y. B. Shin, H. S. Choi, C. S. Lee, S. Kim and M. G. Kim, *Anal Chim Acta*, 2008, **630**, 168-173.
41. M. Canovi, J. Lucchetti, M. Stravalaci, S. Valentino, B. Bottazzi, M. Salmona, A. Bastone and M. Gobbi, *Sensors-Basel*, 2014, **14**, 10864-10875.
42. M. J. Kwon, J. Lee, A. W. Wark and H. J. Lee, *Analytical Chemistry*, 2012, **84**, 1702-1707.

43. X. Hong and E. A. H. Hall, *Analyst*, 2012, **137**, 4712-4719.
44. N. Zhang and D. H. Appella, *Journal of the American Chemical Society*, 2007, **129**, 8424-8425.
45. J. Y. Liu, S. J. Tian, L. Tiefenauer, P. E. Nielsen and W. Knoll, *Analytical Chemistry*, 2005, **77**, 2756-2761.
46. L. Q. Chu, R. Forch and W. Knoll, *Angew Chem Int Edit*, 2007, **46**, 4944-4947.
47. R. D'Agata, G. Breveglieri, L. Zanoli, M. Borgatti, G. Spoto and R. Gambari, *Int J Mol Med*, 2010, **26**, S61-S61.
48. R. D'Agata, R. Corradini, G. Grasso, R. Marchelli and G. Spoto, *Chembiochem*, 2008, **9**, 2067-2070.